Research article

Applicability of waste foundry sand stabilization by fly ash geopolymer under ambient curing conditions

Ali Abdulhasan Khalaf [a,b,*], Katalin Kopecskó [a], Sarah Modhfar [c]

[a] *Department of Engineering and Geotechnics, Faculty of Civil Engineering, Budapest University of Technology and Economics, Muegyetem Rakpart 3, H-1111, Budapest, Hungary*
[b] *Department of Civil Engineering, College of Engineering, University of Basrah, 61004, Basra, Iraq*
[c] *Avicenna E-Learning Center, University of Basrah, 61004, Basra, Iraq*

A B S T R A C T

Recently, utilizing industrial waste in the construction industry has gained significant attention to meet sustainability demands and mitigate the adverse environmental impacts caused by the construction industry. This study evaluates the engineering properties of waste foundry sand as a target material after stabilization with an environmentally friendly stabilizing agent (fly ash geopolymer), focusing on achieving adequate strength under ambient curing conditions as a feasible choice for road bases in geotechnical applications. While fly ash geopolymer application is typically linked with temperature curing, this research explores its application under ambient curing to enhance feasibility and reduce production costs. The fly ash geopolymer was synthesized by activating fly ash using a combination of sodium hydroxide and sodium silicate. The experimental program investigated the geopolymer-stabilized waste foundry sand at varying dosages of 7, 15, and 25 %, examining physical properties, non-destructive tests, mechanical properties, XRD phase analysis, and SEM observation. The results demonstrated that increasing fly ash dosage significantly enhanced the physical properties, mechanical properties, and microstructure of the geopolymer-stabilized waste foundry sand samples. Dry density improved from 1.75 to 2.02 g/cm^3; longitudinal wave velocity increased from 897.3 to 2028.4 m/s, and unconfined compressive strength rose from 109 to 5261 kPa. Notably, only samples with 25% fly ash achieved the requisite strength to satisfy the road base limit (4100 kPa). These outcomes instill confidence in the potential use of waste foundry sand as a construction material and transition it from mere filling material to a valuable resource, furthermore encouraging the adoption of fly ash geopolymer as an environmentally friendly stabilizing agent in geotechnical applications.

1. Introduction

The growing emphasis on environmental preservation and the adoption of eco-friendly approaches is increasingly important. This is driven by the urgent need to reduce the reliance on finite natural resources and advocate for a sustainable future. The global issue of

* Corresponding author. Department of Engineering and Geotechnics, Faculty of Civil Engineering, Budapest University of Technology and Economics, Muegyetem Rakpart 3, H-1111, Budapest, Hungary.

E-mail addresses: ali.abdulhasan.khalaf@emk.bme.hu (A.A. Khalaf), kopecsko.katalin@emk.bme.hu (K. Kopecskó), sara@avicenna.uobasrah.edu.iq (S. Modhfar).

climate change further highlights the necessity of identifying alternative, sustainable resources and adopting practices that minimize harmful effects on the natural environment. Consequently, the field of sustainability science must continuously evolve to enhance ecosystem preservation and contribute to establishing a more sustainable society [1]. Circular economy principles are pertinent for achieving sustainable development goals. It is widely recognized that the transition from a linear economic model to a circular one, characterized by the "produce-use-reuse-recycle" framework, offers a viable solution to prevent the depletion of natural resources and is essential for ensuring a sustainable future. Its primary strategies are anticipated to make a significant contribution towards more effectively managing the substantial quantities of waste in the ecosystem by reducing, reusing, recycling, redesigning, remanu-facturing, and recovering [2–4]. Construction waste, which constitutes 35%–40% of waste generated globally, poses a significant threat to the global economy and sustainability. Such waste materials are primarily inert and non-biodegradable, making them ideal for reuse in the construction sector [5].

Waste foundry sand (WFS) is a by-product of metal foundry industries. It was initially utilized as a casting mold material, but it eventually degraded into finer particles due to the high temperature in the metal foundry process [6]. Manufacturing One ton of metal foundry produces approximately one ton of WSF [6,7]. So far, only 10% of WFS has been recycled in different applications [6,8]. The primary challenge in recycling WFS lies in its classification as poorly graded sand (SP), which characterizes it as problematic soil. Towards sustainable goals, the consumption of primary natural resources can be minimized by recycling and maintaining construction materials simultaneously [8]. Such soil can be employed in geotechnical construction through soil improvement techniques. Portland cement is highly known for stabilizing foundation soils of highways to be used as subgrade, subbase, and base materials [9–12]. From a sustainable point of view, Portland cement is considered an unfriendly environmental material. Its production generates high emis-sions of CO_2 [13]. Approximately one ton of Portland cement production emits one ton of CO_2. This high carbon footprint from the cement industry was attributed to the substantial fuel consumption during clinker production and the decarbonization of lime [13,14]. Towards green cement production, geopolymers have been merged as competitive alternatives to Portland cement, offering a lower carbon footprint while maintaining comparable properties to Portland cement [15,16].

Geopolymers, a class of inorganic polymers, are produced by the reaction of aluminosilicate in an alkaline medium to form a three-dimensional structure. This process involves a series of reactions, starting from aluminosilicate dissolution and ending with the polycondensation of monomers [17]. The aluminosilicate precursors can be manufactured by calcining natural clay minerals at various temperatures (typically 400–800 °C for 2–6 h), producing materials like metakaolin (MK) [18] or by utilizing industrial waste ma-terials rich in aluminosilicates such as fly ash (FA) and ground granulated blast furnace slag (GGBFS) [15]. The alkaline environment is achieved by adding alkali substances such as sodium hydroxide (NaOH), sodium silicate (Na_2SiO_3) or a combination of both [19,20]. The soil improvement applications of FA geopolymers were previously hindered by the assumption that the reaction could only occur when cured with heat (typically 50–80 °C), making it challenging to use in geotechnical practice [21]. However [22], studied the stabilization of soft clay using FA in the geopolymer composition from 20 to 40 activated by sodium hydroxide under ambient curing conditions. Their results were analyzed based on the unconfined compressive strength (UCS) and evaluated by XRD analysis. They concluded that the most significant factor is the concentration of sodium hydroxide, which increases the UCS when it is increased. Furthermore, the increase in water content negatively influenced the results. Another study conducted by Lui et al. [16] investigated the stabilization of loess by FA. The FA geopolymer was activated by sodium or potassium hydroxides under ambient conditions, particularly for road foundations. They first optimized the fly ash geopolymer (FAG) to achieve maximum UCS and subsequently applied the optimal FAG mixture with varying percentages of FA to the loess (10%, 20%, and 30%). The study demonstrated that mechanical properties such as UCS and modulus of elasticity have improved with the increase of FA percentage. In a separate investigation [21] explored the aggregate base improvement by geopolymer synthesized from FA and a combination of FA and red mud with 20% of precursor. They concluded that two crucial factors affect geopolymer performance, curing temperature in a positive impact whereas increased water had a negative impact. Nevertheless, they demonstrated that the ambient curing condition was suf-ficient to develop the required mechanical properties of geopolymer-stabilized base samples and was more practical. Additionally, a study by Ref. [8] examined the properties of WFS to find out that it is poorly-graded sand. The maximum strength is quite low, and its application in construction is limited to low-rise embankment with batter slope.

To date, there is a notable absence of research within existing literature to valorize the waste foundry sand (WFS) as a base material for geotechnical applications. This is largely attributed to its low mechanical properties, restricting its use to low-rise embankments. Thus, the aim of this research is the stabilization of WFS to meet the sustainable demands by (i) employing a green stabilizing agent such as a geopolymer precursor (FA), (ii) activating this precursor by a combination of sodium hydroxide solution (SH) and sodium silicate solution (SS), (iii) executing the stabilization process under ambient conditions, as a feasible application of geopolymer-stabilized WFS bases. The experimental results were evaluated by physical properties, non-destructive tests, mechanical properties, X-ray diffraction (XRD) phase analysis, scanning electron microscopy (SEM) observations and EDS elemental analyses of the geopolymer-stabilized WFS samples.

2. Materials and methods

This section summarizes the source of the WFS and the stabilizing agent properties. In addition, the sample preparation and experimental tests have been explained.

2.1. Source of WFS

The WFS was provided by Wescast Hungary Ltd. (Oroszlány, Hungary). According to the Unified Soil Classification System (USCS),

the boundary between gravel and sand is 4.75 mm [23]. Hence, samples were sieved to pass through a 4.75 mm sieve to remove potentially larger particles mixed with the WFS.

2.2. Fly ash and alkaline activator properties

Fly ash was used as the geopolymer precursor material. The fly ash type Microsit 20 source is Meselia-Hungária Ltd. (Pomáz, Hungary). This type of fly ash is chosen over others because it consists of primarily amorphous and quite fine particles ($d_{95} \leq 20$ μm). Geopolymers with a smaller median particle size precursor gave more reaction products and increased microstructure homogeneity due to fewer non-reacted and non-bridged particles [24]. The chemical composition is made by XRF and presented in Table 1. The particle shape is spherical. The Blain surface and specific gravity are 7300 cm^2/g and 2.38, respectively. Sodium hydroxide solution (SH) was prepared by mixing distilled water with sodium hydroxide pellets of 98% purity to prepare the proper molarity based on the density and temperature [25]. First, the distilled water was put into the flask, and then the pellets were added and gently stirred until they reached homogeneity. The SH was kept for 24 h at the laboratory ambient (20 ± 2 °C) to evolve the reaction heat. The sodium silicate solution (SS) was analytical grade with a silicate modulus (Ms) of 3.16 (% H$_2$O = 65.27, % SiO$_2$ = 26.39, and % Na$_2$O = 8.34). The alkali activator solution (SH + SS) was mixed 24 h prior to used in geopolymer synthesis.

2.3. Sample preparations

Based on the pioneering literature [15,19,22,26] and previous experience [27], the alkaline activator solution (AAS) was fixed at probable optimum controlling factors: molarity of SH = 16 M, SS/SH = 2.0, and w/GPS = 0.2, where w/GPS is the water (w) to geopolymer-solid (GPS) ratio. The WFS was wet by the amount of water (w$_{extra}$) to reach the optimum moisture content (OMC). The fly ash percentages (FA%) regarding the total weight of solids (WFS + FA) were 7, 15, and 25%. The upper limit was selected to be just below the binder percentage in mortar (27%) [28]. The lower limit was chosen by trial in the laboratory that can hold the WFS particles in the sand. Since there is one variable parameter (FA%), the effect is assumed to be a linear relationship [29], and an intermediate value (15%) is chosen to validate this assumption. The detail of the mix proportion is presented in Table 2. First, the geopolymer gel was prepared by adding AAS to FA and mixing for 3.0 min to prepare each mix. Then, the geopolymer gel was added to the wet WFS and continued mixing for a further 4.0 min to achieve a sufficiently homogenized mixture. Eventually, the mixture was poured into three compacted layers in 40*40*80 mm prism molds with a twice-width-to-hight ratio to eliminate the end effects during unconfined compression tests. After 24 h, the samples were de-molded and wrapped with plastic films and then kept under ambient laboratory curing (20 ± 2 °C) until testing at seven days. Three specimens represented each sample, and the average was taken. In the sample IDs, WFS stands for waste foundry sand, FAG stands for fly ash geopolymer, and the numbers are the fly ash (FA) percentages related to the total weight of solids (WFS + FA) (Table 2).

2.4. Testing methods

Physical properties: bulk and dry densities were evaluated for the intact geopolymer-stabilized WFS samples following ASTM D7263 [30], while specific gravity and void ratio were determined by following ASTM D854 [31]. The calculations were obtained by applying Eq. 1- 4 as follows:

$$\gamma_b = (M_t / V_t) \tag{1}$$

$$\gamma_d = (\gamma_b / (1+m)) \tag{2}$$

$$GS = (\gamma_s / \gamma_w) \tag{3}$$

$$e = ((GS * \gamma_w - \gamma_d) / \gamma_d) \tag{4}$$

where γ_b is the bulk density, M_t is the total mass in grams, V_t is the total volume in cm^3, γ_d is the dry density, m is the moisture content in %, GS is the specific gravity, γ_s is the solid density calculated by the pycnometer method, γ_w is the distilled water density, and e is the void ratio.

Non-destructive tests: longitudinal and shear wave velocities were used to evaluate the integrity of the intact geopolymer-stabilized WFS samples following the ASTM C597 [32]. Traveling time (t) of wave propagation through a sample length (l) was measured by an ultrasonic measurement instrument type GEOTRON-ELEKTRONIC of 50 kHz frequency. The instrument is aided by special software that captures the traveling time of longitudinal and shear waves. Both longitudinal wave velocity (V_p) and shear wave velocity (V_s) were calculated by Eqs. (5) and (6) as follows:

Table 1
The chemical composition of fly ash.

Oxide composition	SiO$_2$	Al$_2$O$_3$	Fe$_2$O$_3$	CaO	K$_2$O	LOI[a]
wt.%	52.0	35.7	6.4	2.9	0.6	2.4

[a] : Loss on ignition.

Table 2
Mix proportion of geopolymer-stabilized WFS.

Sample ID	FA %	FA (g)	WFS (g)	SH (g)	SH (M)	SS (g)	w/GPS	w_{extra} (g)	OMC %
WFS_FAG_7	7	105	1395	12.0	16	24	0.2	160.5	13.2
WFS_FAG_15	15	225	1275	25.7	16	51.4	0.2	117.8	13.2
WFS_FAG_25	25	375	1125	42.7	16	85.4	0.2	64.5	13.2

$$V_p = l/t_p \qquad (5)$$

$$V_s = l/t_s \qquad (6)$$

where t_p and t_s are the traveling times of longitudinal and shear waves, respectively.

Mechanical properties: unconfined compressive strength (UCS) and modulus of elasticity (E) testing procedures of geopolymer-stabilized WFS samples were selected to be compatible with cemented soils following the ASTM D5102 [33]. The samples were compressed by a 0.21%/min strain rate using a computer-aided compression machine type INSTRON of 30 kN capacity. The displacement increment was automatically recorded for every load step. The UCS values were determined by dividing the ultimate load by cross-sectional area. The E values were determined by taking the slope at 50% of UCS [34].

Phase analysis: X-ray diffraction (XRD) was conducted to investigate the phase composition of original WFS and geopolymer-stabilized WFS samples. For XRD, the samples were ground manually in a mortar and then sieved with a 44 μm opening size sieve. The ground powder samples were analyzed by PANalytical X'Pert Pro XRD device equipped with a Cu Kα source.

Microstructural investigation: scanning electron microscopic (SEM) observation was conducted on the original WFS and geopolymer-stabilized WFS samples. The original WFS was observed without any modification. The geopolymer-stabilized WFS sample was taken from fragments of specimens after UCS tests with dimensions of about 10 mm long and 3 mm thick. The microstructure of the internal surface of failure due to the UCS test was investigated. The samples were gold-coated under 40 bar vacuum pressure and then investigated using Phenom XL Desktop SEM/EDS. Fig. 1 illustrates the schematic description of the conducted experimental tests.

3. Results and discussion

3.1. Characterization of WFS

The particle size distribution of the WFS is presented in Fig. 2. The majority of WFS particles passed through a 425 μm sieve, demonstrating a coefficient of curvature of 1.2 and a coefficient of uniformity of 2.0. As per the USCS [23], the WFS was classified as poorly graded sand (SP). The specific gravity, as determined by the pycnometer method [31], was found to be 2.59. The standard compaction test was conducted according to Ref. [35] to determine the maximum dry density and optimum moisture content, resulting in values of 1.7 g/m^3 and 13.2 %, respectively. XRD analysis of WFS revealed that the predominant presence of WFS contains mainly a well-crystallized quartz (Q) phase, as shown in Fig. 3. The morphology and elemental composition of WFS were determined by SEM-EDS analysis, as illustrated in Fig. 4. This analysis demonstrated that WFS primarily consisted of oxygen (O) and silicon (Si), constituting approximately 99% by weight, with traces of other elements that may be attributed to the metal casting process in the foundry.
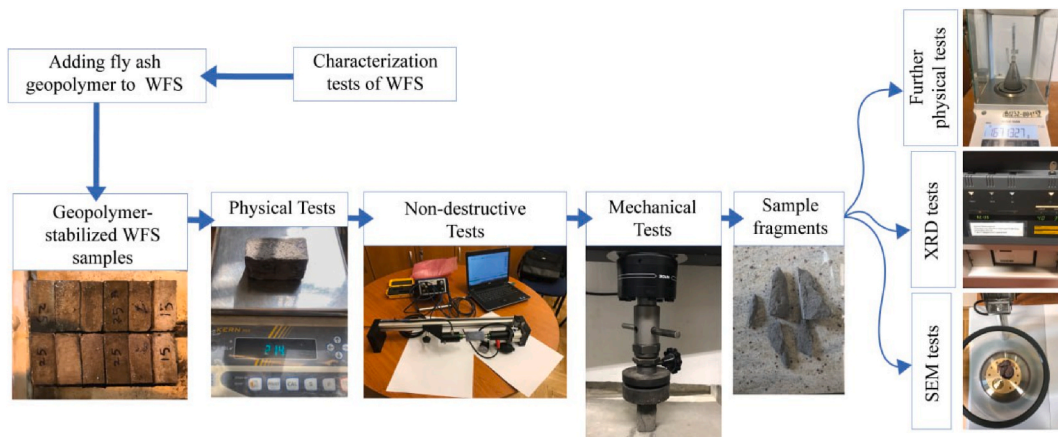
Fig. 1. Scheme of the conducted experimental tests.
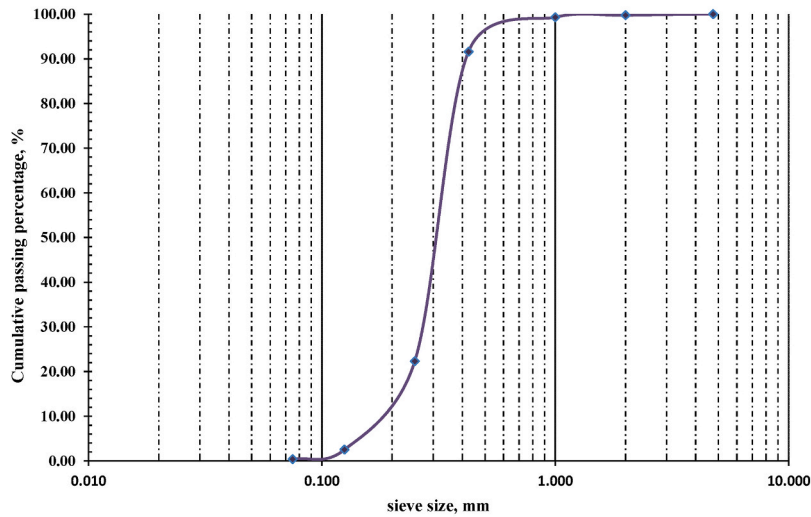
Fig. 2. Particle size distribution curve of WFS.
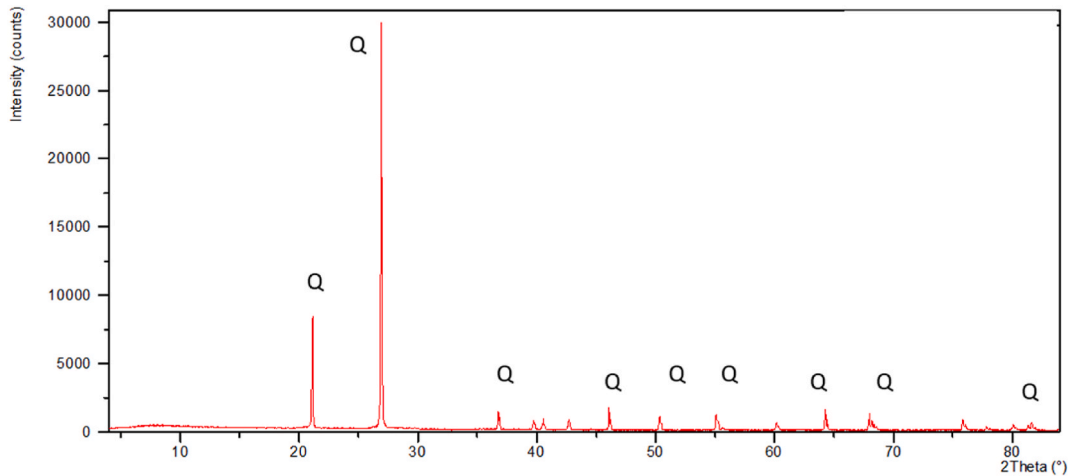
Fig. 3. XRD pattern of WFS, Q: α-quartz.

3.2. Physical properties

The average values of Υ_d, GS, and e for all geopolymer-stabilized WFS samples (WFS_FAG_7, WFS_FAG_15, and WFS_FAG_25) are illustrated in Fig. 5. The additional percentage of FA has a discernible influence on all physical properties, resulting in notable enhancement. Specifically, as FA percentage rises from 7 to 25, it is evident that Υ_d and GS for WFS_FAG_7 and WFS_FAG_25 have exhibited noticeable improvements, increasing from 1.75 to 2.02 g/cm^3 and from 2.40 to 2.45, respectively. These improvements are substantiated by high correlation values ($R^2 = 0.9293$ and 0.9868, respectively). The values of e have seen a considerable reduction, declining from 37.20 % for WFS_FAG_7 to 21.27 % for WFS_FAG_25, with a notably high correlation value ($R^2 = 0.9123$). Consequently, it can be deduced that the augmentation of FA percentage positively impacts the physical properties by simultaneously increasing Υ_d and GS while decreasing e. This transformation creates a denser and more cohesive characteristic of WFS, which is a pivotal initial step in producing a stable base foundation. These results align with prior literature, which has advocated that the properties of WFS could improve by incorporating finer particles [8]. Moreover, Liu et al. [16], proposed that geopolymer has a high efficiency in soil stabilization since the unreacted particles act as micro fillers. On the other hand, reacted geopolymer particles after hardening were considered nanoparticles [36]. Thus, the synergy between the grading of unreacted particles and the fineness of hardened fly ash geopolymer increases WFS stabilization effectiveness when employing fly ash geopolymer.

Display name	Standard data	Quantification method	Result Type
Spc_004	Standardless	ZAF	Metal
Element	Line	Mass%	Atom%
O	K	56.20±0.08	69.27±0.10
Na	K	0.16±0.01	0.14±0.01
Mg	K	0.06±0.00	0.05±0.00
Al	K	0.58±0.01	0.43±0.01
Si	K	42.78±0.04	30.04±0.03
Fe	K	0.12±0.00	0.04±0.00
Cu	K	0.09±0.01	0.03±0.00
Total		100.00	100.00
Spc_004			Fitting ratio 0.0144
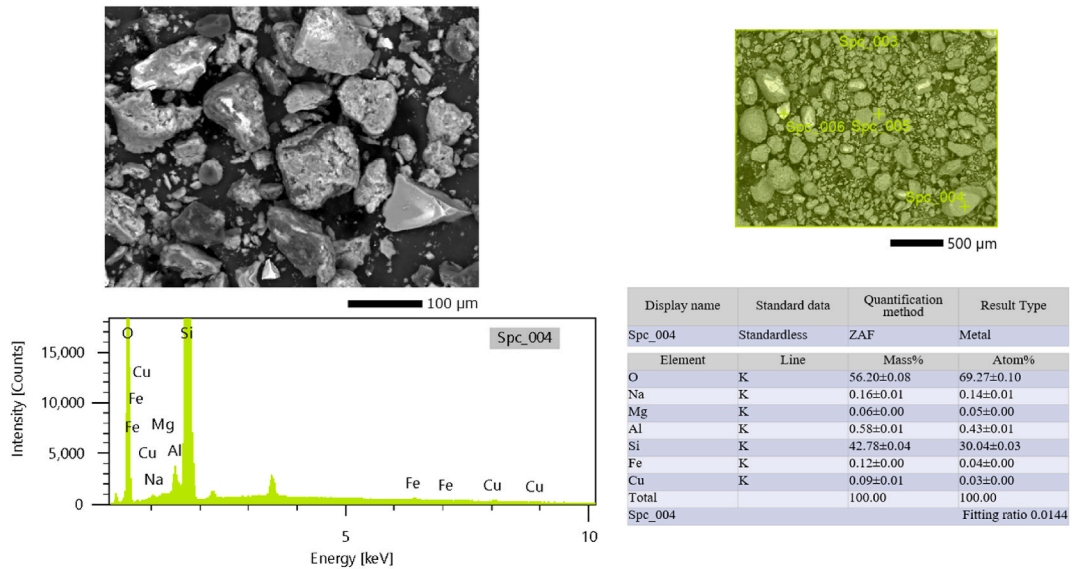
Fig. 4. SEM images (above left) and SEM image with the spots of EDS elemental analysis (above left); spectrum and data of EDS elemental analysis (down) of WFS, Spc_4: Selected particle of WFS.
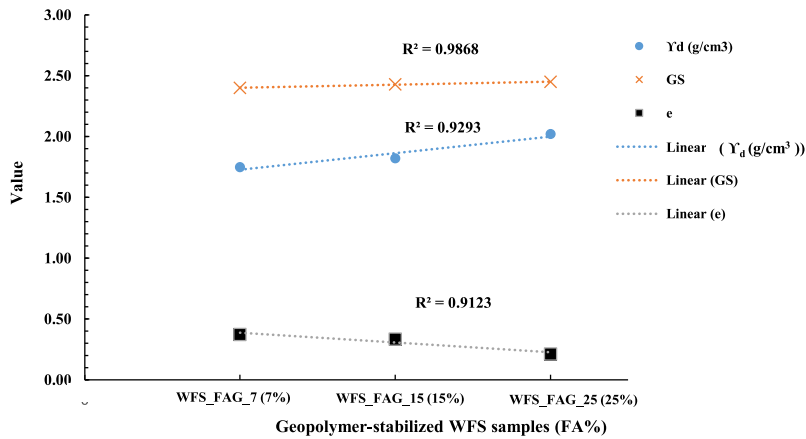
Fig. 5. Effect of FA% on physical properties of geopolymer-stabilized WFS samples.

3.3. Non-destructive tests

The average values of V_p and V_s for all geopolymer-stabilized WFS samples (WFS_FAG_7, WFS_FAG_15, and WFS_FAG_25) are displayed in Fig. 6. Notably, increasing the FA percentage from 7% to 25% yielded a significant enhancement in both V_p and V_s, with V_p increasing from 897.3 to 2028.4 m/s and V_s rising from 574.2 to 1200.5 m/s, respectively. The strong relationship between FA percentage and the velocity waves (V_p and V_s) is highlighted by the high R^2 values, which stand at 0.9004 and 0.9096, respectively, as depicted in Fig. 6. To obtain a better perspective on the results, the V_p and V_s values were compared to those of sandstone [18]. This comparison revealed that only one sample (WFS_FAG_25) was within the range of the sandstone results [18], signifying its equivalence in terms of integrity. Conversely, samples with 7% and 15% FA exhibited lower integrity compared to sandstone. WFS_FAG_7 and WFS_FAG_15 samples had considerably lower values of Υ_d (1.82 g/cm³ and 1.75 g/cm³) along with higher e values (37.20% and 33.52%), in contrast to WFS_FAG_25 sample, which exhibited a higher Υ_d value of 2.02 g/cm³ and a lower e value of 21.27%. At this point, the non-destructive tests were able to characterize the WFS_FAG_25 sample as a good-quality sample since it has V_p and V_s values comparable to sandstone [18]. Interestingly, sandstone is widely used during the construction of road bases [37]. Sample WFS_FAG_25, being as good as sandstone, can successfully be used as a sustainable base material for roads.
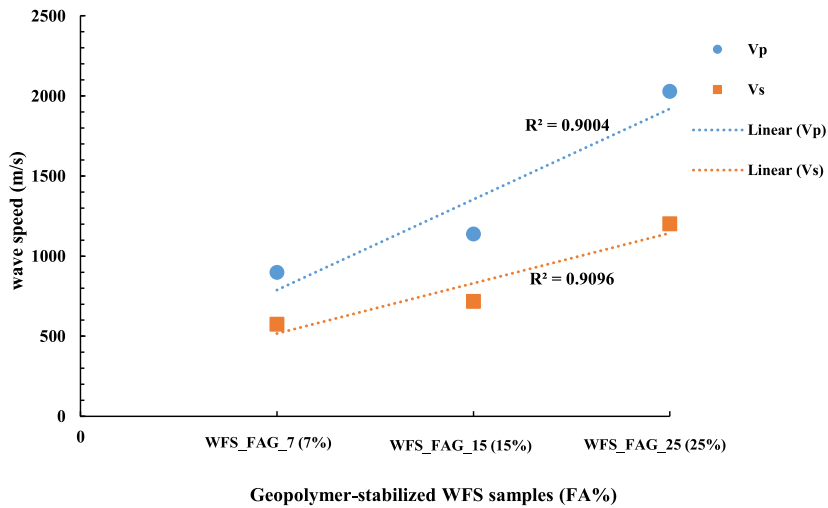
Fig. 6. Non-destructive results of geopolymer-stabilized WFS samples.

3.4. Mechanical properties

The WFS has previously been classified as poorly-graded sand, known for its low mechanical properties [8]. Thus, the mechanical tests conducted in this study focused on investigating the feasibility of using the geopolymer-stabilized WFS as a stabilized sand material. There was no direct comparison of mechanical properties between the original soil (WFS) and geopolymer-stabilized WFS.

The UCS and E values of all geopolymer-stabilized WFS samples subjected to ambient curing for seven days are displayed in Figs. 7 and 8, respectively. Fig. 7 indicates that UCS values have a strong correlation and increase with the addition of FA percentage. This behavior can be attributed to geopolymer gel providing considerable cohesion between WFS particles and contributing to strength. It is noticeable that only the WFS_FAG_25 sample has passed the required UCS value for use as a base material [38], as illustrated in Fig. 7. This result is consistent with non-destructive tests, which suggested that only the WFS_FAG_25 sample can be characterized as a good-quality sample. In a related study [16], examined the stabilization of loess with FA for potential use in road bases. Their results yielded a maximum UCS of 4300 kPa for 30% of FA activated by SS and SH. In this research, the geopolymer-stabilized WFS with 25% of FA activated by SS and SH achieved a UCS of 5261 kPa, as shown in Fig. 7. Therefore, geopolymer-stabilized WFS with 25% of FA is eligible to be used as road bases.

Fig. 8 presents the E values of geopolymer-stabilized WFS samples. It shows that E increases with the addition of FA percentage. This increase is attributed to the growing quantity of synthesized geopolymer surrounding the WFS particles. The E values for the WFS_FAG_7 and WFS_FAG_15 samples (32.30 MPa and 43.62 MPa, respectively) are comparable and relatively low compared to the E value of the WFS_FAG_25 sample (588.98 MPa); this is because the geopolymer gel is insufficient to bind all WFS particles for 7 and 15 % of FA. Therefore, 25% of FA is the practically perfect percentage to meet the minimum requirement of UCS for base materials and a relatively high value of E. These results agree with existing literature findings that increasing the geopolymer content increases E values, as it enhances homogeneity and produces a more uniform structure frame that holds the soil particles [16]. Furthermore, increasing the FA percentage leads to an increase in fine particles, which can improve the grading of the poorly-graded WFS [8].
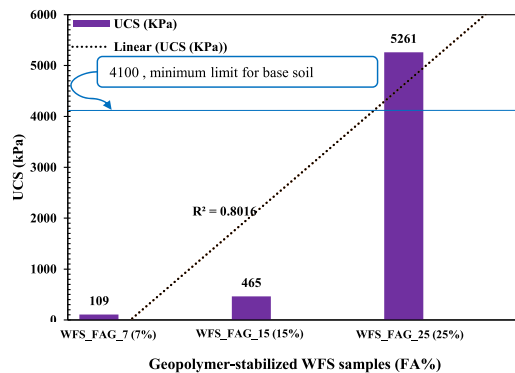
Fig. 7. UCS values of geopolymer-stabilized WFS samples.
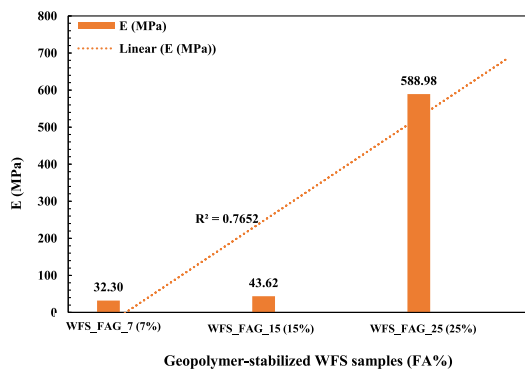
Fig. 8. E values of geopolymer-stabilized WFS samples.

Stress-strain curves and failure modes of representative specimens of WFS_FAG_7, WFS_FAG_15, and WFS_FAG_25 samples are shown in Fig. 9(a–f). According to Ref. [33], the failure modes of cemented soils can indicate either a barrel, cylindrical or brittle failure modes. All geopolymer-stabilized WFS samples showed a brittle failure mode. This kind of failure mode was also reported in the literature for cemented soils [39]. The brittleness was increased when the FA percentage was higher. This behavior can be attributed to the nature of geopolymer, which has a brittle fracture [40].

3.5. XRD analysis

The XRD analysis was conducted on geopolymer-stabilized WFS samples for further investigations, as illustrated in Fig. 10. Notably, there is a broad hump at XRD patterns for all geopolymer-stabilized WFS samples from 5° to 32° 2Theta. This broad hump in XRD patterns is associated with the presence of amorphous phases and detects the geopolymer synthesis, as referenced in previous studies [16,41]. By observing these XRD patterns, all geopolymer-stabilized WFS samples show identical XRD patterns with two discernible crystalline phases: α-quartz (Q) and mullite (M). By comparing these results with the XRD patterns of the original WFS (Fig. 3) and fly ash geopolymer in Fig. 11, it can be inferred that the crystalline phase M in the geopolymer-stabilized WFS samples likely originates from unreactive FA. No new observable crystalline phases emerged during the stabilization process with varying FA dosages. Although the percentage of dosage was different, the mineral composition was stable; this is evidence that WFS does not react with the stabilizing agent. It is reported that silica quartz can only participate in the geopolymerization reaction when the curing temperature exceeds 800 °C [17]. In this research study, the curing temperature is kept at ambient condition (20 ± 2 °C), and the chemical composition of WFS primarily consists of silica quartz. Therefore, it is unsurprising that the XRD patterns of geopolymer-stabilized WFS samples remain consistent, indicating no further reaction between WFS and the stabilizing agent. This behavior is different from clayey soils, such as expansive soils that tend to react with stabilizing agents [42]. Therefore, it can be confidently confirmed that the key factor in enhancing the geopolymer-stabilized WFS is the percentage of FA addition, which provides sufficient geopolymer gel to bind the WFS particles, providing the cohesion characteristic as observed in WFS_FAG_25 sample that exhibits superior properties over WFS_FAG_15 and WFS_FAG_7 samples.

3.6. SEM analysis

Mechanical tests, including non-destructive tests, have demonstrated that only the WFS_FAG_25 sample fulfilled the requirements as a base material. Furthermore, the XRD analysis revealed that the detectable crystalline phase composition is identical for all geopolymer-stabilized WFS samples. Thus, the SEM analysis has been performed to investigate the microstructure of the WFS_FAG_25 sample. The microstructure of the WFS_FAG_25 sample is depicted in Fig. 12. The SEM image of the WFS_FAG_25 sample clearly indicates that the WFS particle is encapsulated by FA geopolymer (FAG). Some microcracks are visible, which may have developed either during the mechanical test or due to shrinkage [16]. The micropores appear to be filled with FAG to some extent. A large surface area of the WFS particle is surrounded by FAG, thus enhancing the strength by providing cohesion due to the binding behavior of FAG. This microstructure is found to be similar to the microstructure observed in dredged sediment stabilized by cement [43]. The FAG microstructure shows some unreacted and partially reacted particles. This result aligns with [16], who suggested that the unreacted particles of FA behave as microfillers. Therefore, increasing the FA percentage increases the homogeneity of the structure frame to produce more stable and coherent soil suitable for road bases.

4. Conclusion

In this study, fly ash (FA) geopolymer was utilized to improve waste foundry sand (WFS) behavior, which can serve as a stabilized sand base material. Fly ash geopolymer was synthesized by activating fly ash with a combination of sodium hydroxide and sodium silicate solutions, hardening under ambient curing conditions. Heat treatment was not applied for practical reasons. Three FA
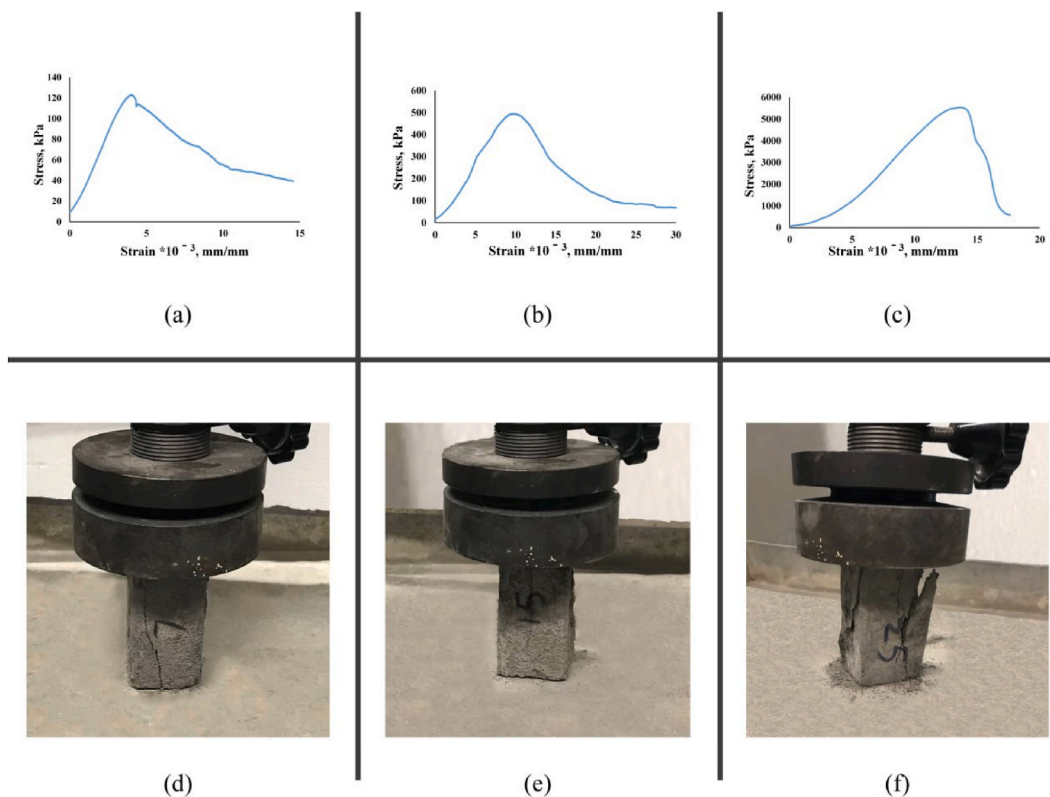
Fig. 9. Stress-strain curves and failure modes of geopolymer-stabilized WFS representative specimens. a. Stress-strain curve of WFS_FAG_7; b. Stress-strain curve of WFS_FAG_15; c. Stress-strain curve of WFS_FAG_25; d. The failure mode of the stress-strain curve of WFS_FAG_7; e. The failure mode of the Stress-strain curve of WFS_FAG_15; f. The failure mode of the stress-strain curve of WFS_FAG_25.

percentages (7, 15 and 25 %) were applied to produce geopolymer-stabilized WFS. All samples were investigated by physical, non-destructive, and mechanical tests for the adequacy of base material requirements, and the microstructure was evaluated based on XRD and SEM analyses.

The test results confirmed that the physical and mechanical properties notably improved when the FA percentage increased in the composition of the FA geopolymer-stabilized WFS. Dry density improved from 1.75 to 2.02 g/cm^3; longitudinal wave velocity increased from 897.3 to 2028.4 m/s, and unconfined compressive strength rose from 109 to 5261 kPa. The non-destructive test results showed that the WFS_FAG_25 sample exhibited significantly higher wave velocities compared with the WFS_FAG_7 and WFS_FAG_15 samples, indicating the robust integrity of the WFS_FAG_25 sample. The strength development of geopolymer-stabilized WFS was adequate for base material requirements only when a 25% FA was incorporated in the WFS_FAG_25 sample. Both WFS_FAG_7 and WFS_FAG_15 samples developed poor strength due to an insufficient amount of stabilizing agents in the mixtures. The XRD analysis further revealed that all geopolymer-stabilized WFS samples displayed identical patterns of crystalline phases. The SEM analysis demonstrated that geopolymer-stabilized WFS had a stable and compact microstructure due to geopolymer synthesis. These findings strongly indicate that the engineering properties of geopolymer-stabilized WFS samples enhanced due to the binding characteristic of geopolymer gel. To look towards potential applications and future directions, geopolymer-stabilized WFS emerges as an environmentally apprehensive solution for sustainable construction. It facilitates utilizing waste materials while minimizing the carbon footprint associated with traditional stabilizing agents. The practical implications of the geopolymer-stabilized WFS satisfy the requirement both for subgrades and road bases. Moreover, this innovative approach could be theoretically extended to a wider range of geotechnical applications that require relatively low strength, such as pipeline bases.

5. Limitations and future work

This research study is limited to utilizing fly ash as the geopolymer precursor and a combination of sodium hydroxide solution and sodium silicate solution as an alkali activator to stabilize waste foundry sand, specifically for road base applications. In light of future endeavors, the authors recommend investigating alternative geopolymer precursors and different combinations of alkali activators, such as potassium hydroxide solution and potassium silicate solution to stabilize waste foundry sand.
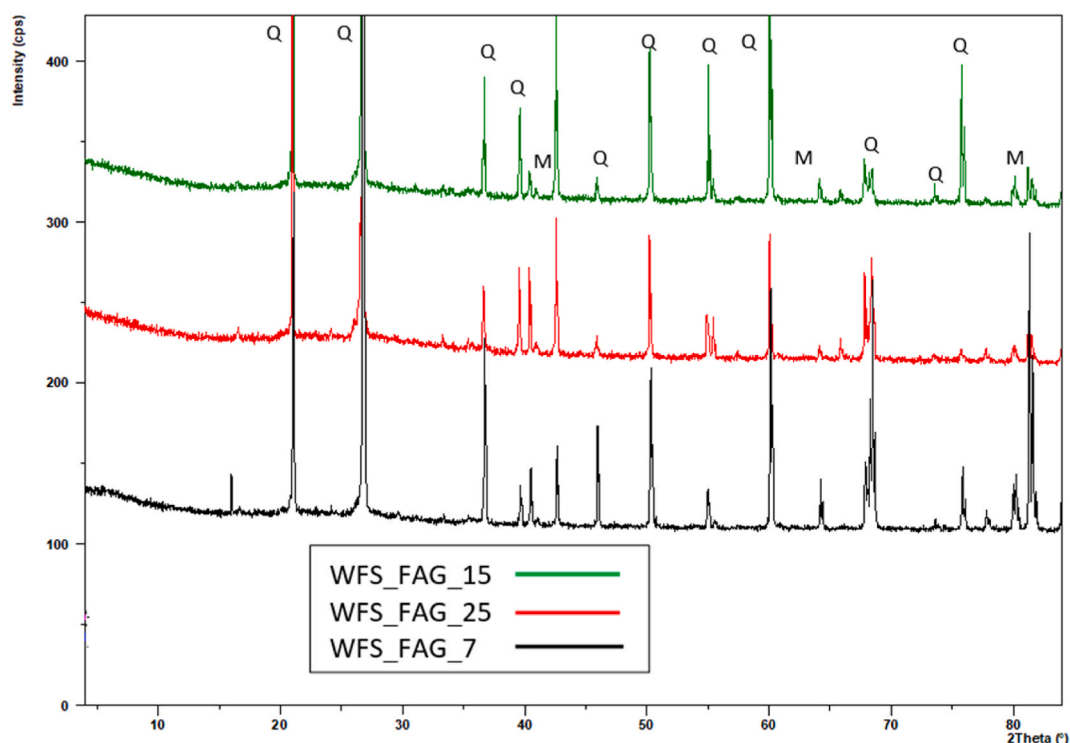
Fig. 10. The XRD patterns of geopolymer-stabilized WFS samples, Q: α-quartz and M: mullite.
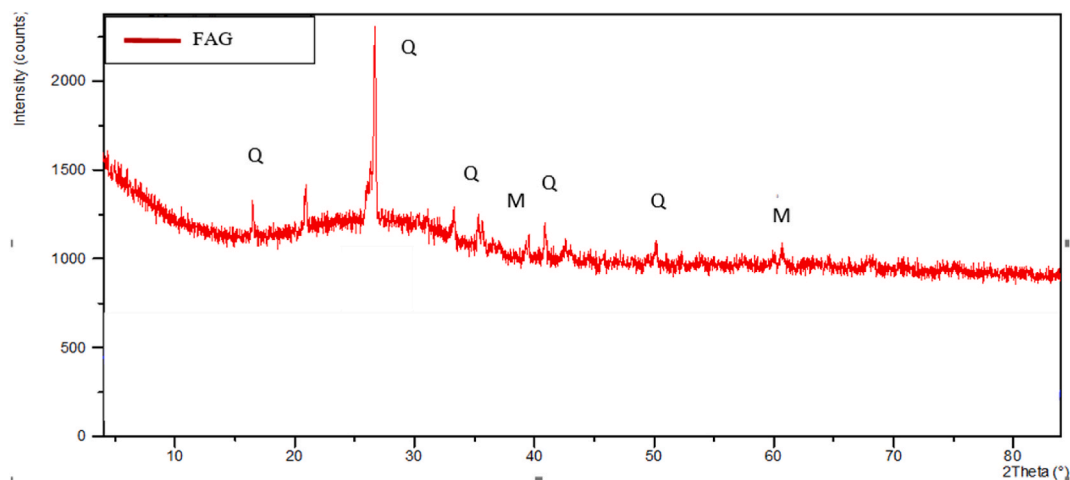
Fig. 11. The XRD pattern of fly ash geopolymer (FAG), Q: quartz and M: mullite.

Data availability statement

Data included in the article.

CRediT authorship contribution statement

Ali Abdulhasan Khalaf: Writing – review & editing, Writing – original draft, Visualization, Validation, Software, Methodology, Investigation, Funding acquisition, Formal analysis, Data curation, Conceptualization. **Katalin Kopecskó:** Writing – review & editing, Writing – original draft, Validation, Supervision, Resources, Project administration, Funding acquisition, Formal analysis, Data curation, Conceptualization. **Sarah Modhfar:** Writing – review & editing, Writing – original draft, Visualization, Software, Investigation, Formal analysis, Data curation, Conceptualization.
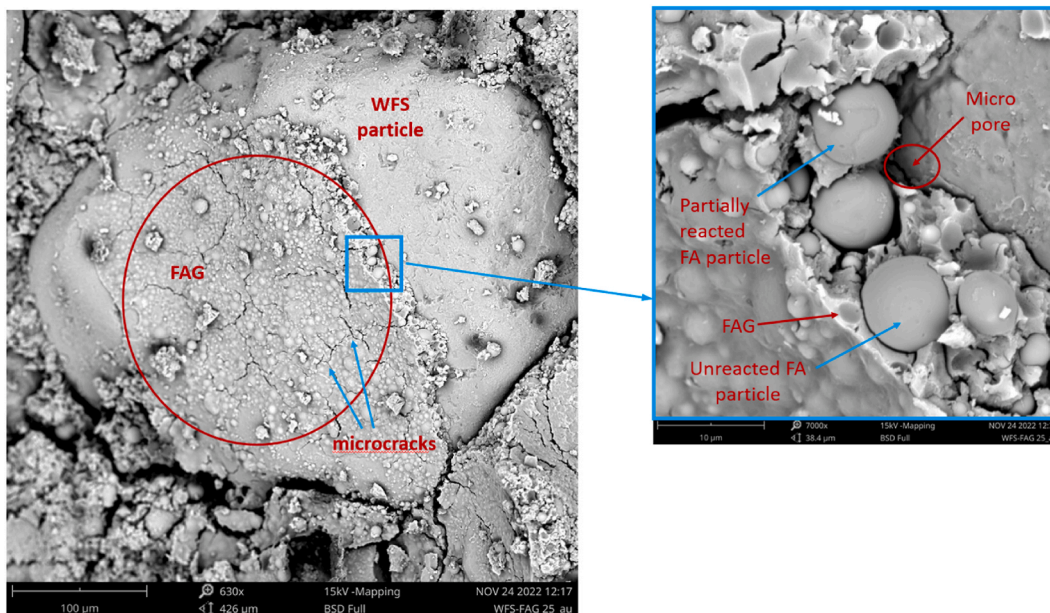
Fig. 12. SEM images of the geopolymer-stabilized WFS.

Declaration of competing interest

The authors declare that they have no known competing financial interests or personal relationships that could have appeared to influence the work reported in this paper.

Acknowledgements

References

[1] G. Silveira, M. Lorena, F. Martins, A. Cesar, S. Bezerra, F. Gabriel, Ecological geopolymer produced with a ternary system of red mud, glass waste , and Portland cement 6 (2022) 1–14, https://doi.org/10.1016/j.clet.2021.100379.

[2] P. Schröder, M. Oyinlola, J. Barrie, B. Fwangkwal, S. Abolfathi, Making policy work for Africa's circular plastics economy, Resour. Conserv. Recycl. 190 (2023) 2022–2024, https://doi.org/10.1016/j.resconrec.2023.106868.

[3] M. Oyinlola, O. Kolade, P. Schröder, V. Odumuyiwa, B. Rawn, K. Wakunuma, S. Sharifi, S. Lendelvo, I. Akanmu, R. Mtonga, et al., A Socio-Technical perspective on transitioning to a circular plastic economy in Africa, SSRN (2023) 1–59, https://doi.org/10.2139/ssrn.4332904.

[4] O. Kolade, V. Odumuyiwa, S. Abolfathi, P. Schröder, K. Wakunuma, I. Akanmu, T. Whitehead, B. Tijani, M. Oyinlola, Technology acceptance and readiness of stakeholders for transitioning to a circular plastic economy in Africa, Technol. Forecast. Soc. Change (2022) 183, https://doi.org/10.1016/j.techfore.2022.121954.

[5] M.S. Jain, A mini review on generation, handling, and initiatives to tackle construction and demolition waste in India, Environ. Technol. Innovat. 22 (2021) 101490, https://doi.org/10.1016/j.eti.2021.101490.

[6] M. Heidemann, H.P. Nierwinski, D. Hastenpflug, B.S. Barra, Y.G. Perez, Geotechnical behavior of a compacted waste foundry sand, Construct. Build. Mater. 277 (2021) 122267, https://doi.org/10.1016/j.conbuildmat.2021.122267.

[7] M. Zanetti, A. Godio, Recovery of foundry sands and iron fractions from an industrial waste landfill, Resour. Conserv. Recycl. 48 (2006) 396–411, https://doi.org/10.1016/j.resconrec.2006.01.008.

[8] E. Yaghoubi, A. Arulrajah, M. Yaghoubi, S. Horpibulsuk, Shear strength properties and stress–strain behavior of waste foundry sand, Construct. Build. Mater. 249 (2020) 118761, https://doi.org/10.1016/j.conbuildmat.2020.118761.

[9] T. Hata, A. Clarà Saracho, A. GuhaRay, S. Kenneth Haigh, Strength characterization of cohesionless soil treated with cement and polyvinyl alcohol, Soils Found. (2022) 62, https://doi.org/10.1016/j.sandf.2022.101238.

[10] S. Yoon, M. Abu-Farsakh, Laboratory investigation on the strength characteristics of cement-sand as base material, KSCE J. Civ. Eng. 13 (2009) 15–22, https://doi.org/10.1007/s12205-009-0015-x.

[11] E.I. Stavridakis, Evaluation of engineering and cement-stabilization parameters of clayey-sand mixtures under soaked conditions, Geotech. Geol. Eng. 23 (2005) 635–655, https://doi.org/10.1007/s10706-004-0800-8.

[12] W. Chimoye, B. Ash, Strength behavior of poorly graded sand improved by cement and bagasse ash, Int. J. Eng. Res. Technol. 6 (2017) 288–291.

[13] J. Davidovits, Geopolymer cements to minimize carbon-dioxide greenhouse-warming, Ceram. Trans. 37 (1993) 165–182.

[14] C.A. Hendriks, E. Worrell, L. Price, N. Martin, L. Ozawa Meida, D. de Jager, P. Riemer, Emission reduction of greenhouse gases from the cement industry, Greenhouse Gas Control Technologies 4 (1999) 939–944.

[15] J.L. Provis, J.S.J. van Deventer, Alkali Activated Materials State-Of-The-Art Report; Springer, vol. 13, Berlin/Heidelberg, Germany, Berlin/Heidelberg, Germany, 2014, 978-94-007-7671-5.
[16] Z. Liu, C.S. Cai, F. Liu, F. Fan, Feasibility study of loess stabilization with fly ash–based geopolymer, J. Mater. Civ. Eng. 28 (2016) 1–8, https://doi.org/10.1061/(asce)mt.1943-5533.0001490.
[17] J. Davidovits, Geopolymers - inorganic polymeric new materials, J. Therm. Anal. 37 (1991) 1633–1656, https://doi.org/10.1007/BF01912193.
[18] M.A. Kassab, A. Weller, Study on P-wave and S-wave velocity in dry and wet sandstones of Tushka region, Egypt, Egyptian Journal of Petroleum 24 (2015) 1–11, https://doi.org/10.1016/j.ejpe.2015.02.001.
[19] D. Hardjito, B.V. Rangan, Development and Properties of Low-Calcium Fly Ash-Based Geopolymer Concrete, Perth, Australia., 2005.
[20] H.H. Abdullah, M.A. Shahin, M.L. Walske, A. Karrech, Cyclic behaviour of clay stabilised with fly-ash based geopolymer incorporating ground granulated slag, Transportation Geotechnics 26 (2021) 100430, https://doi.org/10.1016/j.trgeo.2020.100430.
[21] W. Hu, Q. Nie, B. Huang, A. Su, Y. Du, X. Shu, Q. He, Mechanical property and microstructure characteristics of geopolymer stabilized aggregate base, Construct. Build. Mater. 191 (2018) 1120–1127, https://doi.org/10.1016/j.conbuildmat.2018.10.081.
[22] N. Cristelo, S. Glendinning, L. Fernandes, A.T. Pinto, Effects of alkaline-activated fly ash and Portland cement on soft soil stabilisation, Acta Geotechnica 8 (2013) 395–405, https://doi.org/10.1007/s11440-012-0200-9.
[23] ASTM D2487 Standard Practice for Classification of Soils for Engineering Purposes (Unified Soil Classification System) 1, ASTM International, West Conshohocken, PA, USA, 2011.
[24] S.K. Nath, S. Kumar, Role of particle fineness on engineering properties and microstructure of fly ash derived geopolymer, Construct. Build. Mater. 233 (2020) 117294, https://doi.org/10.1016/j.conbuildmat.2019.117294.
[25] T.T. Nguyen, C.I. Goodier, S.A. Austin, Factors affecting the slump and strength development of geopolymer concrete, Construct. Build. Mater. 261 (2020) 119945, https://doi.org/10.1016/j.conbuildmat.2020.119945.
[26] P. Pavithra, M. Srinivasula Reddy, P. Dinakar, B. Hanumantha Rao, B.K. Satpathy, A.N. Mohanty, A mix design procedure for geopolymer concrete with fly ash, J. Clean. Prod. 133 (2016) 117–125, https://doi.org/10.1016/j.jclepro.2016.05.041.
[27] A.A. Khalaf, K. Kopecsk, I. Merta, Prediction of the compressive strength of fly ash geopolymer concrete by an optimised neural network model, Polymers 14 (2022).
[28] ASTM C109/C109M Standard Test Method for Compressive Strength of Hydraulic Cement Mortars (Using 2-in. Or [50-mm] Cube Specimens), ASTM International, West Conshohocken, PA, USA, 2015.
[29] J. Antony, Full factorial designs, in: Design of Experiments for Engineers and Scientists, Elsevier Ltd: 32 Jamestown Road, London NW1 7BY, 2014, pp. 63–85.
[30] ASTMD7263 Standard Test Methods for Laboratory Determination of Density (Unit Weight) of Soil; ASTM International, West Conshohocken, PA, USA, 2009; Vol. i;.
[31] ASTM D854 Standard Test Methods For Specific Gravity of Soil Solids by Water Pycnometer, ASTM International, West Conshohocken, PA, USA, 2014.
[32] ASTM C597 Standard Specification for Pulse Velocity through Concrete; West Conshohocken, PA, USA, 2009.
[33] ASTM D5102 Standard Test Methods for Unconfined Compressive Strength of Compacted Soil-Lime, ASTM International, West Conshohocken, PA, USA, 2009.
[34] P.K.S. Selvakumar, B.S.A.R. Krishnaraja, Strength enhancement of clay soil stabilized with Ordinary Portland cement , sodium silicate and sodium hydroxide, International Journal of Pavement Research and Technology (2022), https://doi.org/10.1007/s42947-022-00197-4.
[35] ASTM D698 Standard Test Methods for Laboratory Compaction Characteristics of Soil Using Standard Effort (12 400 ft-lbf / ft 3 (600 kN-m / m 3)) 1; ASTM International, West Conshohocken, PA, USA, 2015; Vol. 3;.
[36] J. Geopolymers Davidovits, Ceramic-like inorganic polymers, J. Ceram. Sci. Technol. 8 (2017) 335–350, https://doi.org/10.4416/JCST2017-00038.
[37] H. Li, X. Guo, J. Xin, Y. Li, F. Zhang, G. Zhao, P. Guo, Y. Sheng, Study on the characteristics of sandstone and feasibility to replace limestone in cement stabilized macadam base, International Journal of Pavement Research and Technology (2022), https://doi.org/10.1007/s42947-022-00206-6.
[38] National Concrete Pavement; Center, T, Cement-Stabilized Subgrade Soils, Iowa State, 2020.
[39] F. Ávila, E. Puertas, R. Gallego, Mechanical characterization of lime-stabilized rammed earth: lime content and strength development, Construct. Build. Mater. 350 (2022) 128871, https://doi.org/10.1016/j.conbuildmat.2022.128871.
[40] M. Steinerova, L. Matulova, P. Vermach, J. Kotas, The brittleness and chemical stability of optimized geopolymer composites, Materials 10 (2017), https://doi.org/10.3390/ma10040396.
[41] John L. Provis, Grant C. Lukey, J.S.J. van D, Do geopolymers actually contain nanocrystalline zeolites? A reexamination of existing results john, Am. Chem. Soc. (2005) 3075–3085.
[42] A.A. Khalaf, K. Kopecskó, Utilizing residual red mud by geopolymerization process – from an expansive soil to a rock-like material, Cleaner Engineering and Technology (2023) 14, https://doi.org/10.1016/j.clet.2023.100647.
[43] X. Zhang, D. Li, L. Lang, Evaluation of strength development in cemented dredged sediment admixing recycled glass powder, Construct. Build. Mater. 342 (2022) 127996, https://doi.org/10.1016/j.conbuildmat.2022.127996.